



## Research article

# Influence of pancreaticoduodenectomy for periampullary carcinoma on intestinal microbiome and metabolites

Junwei Fang<sup>1</sup>, Chunhong Xiao<sup>1</sup>, Yafeng Qi, Weixuan Hong, Meiping Wang<sup>\*</sup>*Department of General Surgery, 900th Hospital of Joint Logistics Support Force of People's Liberation Army, Fuzhou, Fujian, 350000, China*

## ARTICLE INFO

**Keywords:**

Pancreaticoduodenectomy  
Intestinal microbiome  
Metabolites  
Choline  
Prevotella  
Prognosis

## ABSTRACT

Recent growing evidence suggests a role for intestinal microbiome and metabolites in patients' postoperative recovery. Therefore, there is a need to gain insight into the impact of pancreaticoduodenectomy for periampullary carcinoma on microbiome and metabolites and the potential impact of their changes on patients' condition. Based on 16S rDNA gene sequencing and untargeted metabolomic analysis, we found that the diversity and abundance of intestinal microbiome were significantly higher in patients preoperatively than postoperatively, and the level of intestinal probiotics was significantly lower after surgery compared with preoperatively. In addition, the choline metabolism level was increased and the amino acid metabolism level was decreased after surgery. A total of 53 differential microbiome and 52 differential metabolites were detected, and the differential metabolites were mapped to approximately 60 different KEGG metabolic pathways, of which 13 KEGG metabolic pathways had a differential metabolite number greater than 5. A total of 88 colony-metabolite pairs with significant positive correlation and 69 colony-metabolite pairs with significant negative correlation were identified. Our results reveal alterations in intestinal microbiome after pancreaticoduodenectomy, suggesting its association with postoperative complications. Moreover, the elevated choline metabolism level in postoperative patients may predict their poorer prognosis. At the same time, the decreased abundance of such probiotic bacteria as *Prevotella* spp. in the postoperative intestine of patients will affect the amino acid metabolism of the organism to some extent.

## 1. Introduction

Currently, intestinal microbiome and metabolites are thought to have a role in disease onset, progression, and postoperative recovery [1–3]. A study of the gut mucosal microbiota showed that microbiota structure was associated with disease recurrence or remission [4]. Several studies have also demonstrated that there is a link between intestinal microbiome and metabolites and postoperative outcomes [5,6]. For example, changes in microbiome and metabolites in gastric cancer patients following gastrectomy have been associated with an increased risk of developing heterochronic colorectal cancer [7,8]. These findings suggest that understanding postoperative changes in intestinal microbiome and metabolites will potentially improve the diagnosis and treatment of diseases and improve patient prognosis.

Pancreatic head cancer, jugular cancer, lower bile duct cancer and duodenal cancer are collectively called periampullary carcinoma

<sup>\*</sup> Corresponding author.

*E-mail address:* [12281982@qq.com](mailto:12281982@qq.com) (M. Wang).

<sup>1</sup> These authors equally contribute to this paper.

[9], which is highly malignant, fast developing, and easy to spread, and there are no obvious symptoms in the early stage, so most patients have already reached advanced stage when they are diagnosed [10], among which pancreatic head cancer is the most serious [11]. This is mainly due to the early infiltration of pancreatic head cancer into the surrounding blood vessels, tissues and organs, and can metastasize along the nerves and lymph, so the mortality rate of patients is extremely high [12], and the median survival period is only 6 months [13], according to statistics, pancreatic cancer may become the second leading cause of cancer death in the world by 2030 [14]. Current cancer treatment usually includes preoperative neoadjuvant therapy, radical surgical resection and postoperative radiotherapy. Neoadjuvant treatment for periampullary cancer may improve the survival rate of patients, but there is no consensus on the specific treatment plan, while postoperative radiotherapy is less effective for its treatment, therefore radical surgical resection is still the most effective means for patients to obtain long-term survival [15].

Pancreaticoduodenectomy, as the primary surgical treatment for periampullary cancer, generally involves resection of pancreatic head, duodenum, distal stomach, gallbladder, and common bile duct, as well as the associated surrounding tissues and organs if they have been invaded, and the most critical factor determining patient survival is whether the tumor is completely removed [16]. However, the effect of pancreaticoduodenectomy on intestinal microbiome and metabolites and the potential impact of its changes on the patient's condition are not known.

Therefore, we performed 16S rDNA gene sequencing and untargeted metabolomic analysis on preoperative and postoperative faecal samples from patients (n = 20). The aim of this study was to gain a comprehensive understanding of the effects of pancreaticoduodenectomy on intestinal microbiome and metabolites with the aim of improving the nutritional status and follow-up examination of postoperative patients.

## 2. Materials and methods

### 2.1. Study subjects and stool sample collection

Twenty patients who were hospitalized in the general surgery department of the 900th Hospital of the Joint Security Forces of the Chinese People's Liberation Army from February 2021 to October 2021 and underwent pancreaticoduodenectomy were screened (Table 1).

Inclusion criteria: surgical treatment modality was pancreaticoduodenectomy; pathologically confirmed diagnosis of peri-pot belly cancer; no chemotherapy or radiotherapy or immunotherapy before surgery; no probiotic or prebiotic taking habit.

Exclusion criteria: suffering from other systemic malignancies; previous history of gastrointestinal surgery; suffering from other gastrointestinal diseases; receiving antibiotic treatment within 1 month.

Fisher's exact test was used for comparisons between groups of categorical variables, and *t*-test was used for comparisons between groups of numerical variables.

**Table 1**  
General information of patients.

characteristics	Male (n = 15)	Female (n = 5)	pvalue
Tumor location, n (%)			0.808
Pancreas	8 (40 %)	3 (15 %)	
Duodenum	3 (15 %)	0 (0 %)	
Bile ducts	4 (20 %)	2 (10 %)	
Jaundice, n (%)			0.260
+	9 (45 %)	5 (25 %)	
-	6 (30 %)	0 (0 %)	
Diabetes, n (%)			1.000
+	2 (10 %)	1 (5 %)	
-	13 (65 %)	4 (20 %)	
Hypertension, n (%)			0.290
+	4 (20 %)	3 (15 %)	
-	11 (55 %)	2 (10 %)	
T stage, n (%)			0.530
T1	5 (25 %)	1 (5 %)	
T2	3 (15 %)	3 (15 %)	
T3	5 (25 %)	1 (5 %)	
T4	2 (10 %)	0 (0 %)	
N stage, n (%)			0.300
N0	9 (45 %)	4 (20 %)	
N1	5 (25 %)	0 (0 %)	
N2	1 (5 %)	1 (5 %)	
Stage, n (%)			0.817
Stage I	7 (35 %)	3 (15 %)	
Stage II	2 (10 %)	1 (5 %)	
Stage III	6 (30 %)	1 (5 %)	
Age, mean ± sd	64.333 ± 5.7155	59.6 ± 15.06	0.527
BMI, mean ± sd	22.44 ± 3.4636	22.28 ± 4.1919	0.933

Faecal sampling time: 3 days before surgery and 7–10 days after surgery. Fresh faecal was collected with a sterile spoon, and the faecal in the middle medial part was strictly scooped as the sample; after the sample was taken, it was put into a sterile preservation tube, the cap was screwed tightly, and the sample was kept in an anaerobic environment and quickly stored at  $-80^{\circ}\text{C}$ . Grouping: preoperative stools were group Q and postoperative stools were group H.

## 2.2. DNA extraction and 16S rDNA amplicon sequencing

The DNA of the samples was extracted using the Magnetic Soil And Stool DNA Kit (TIANGEN) according to the manufacturer's instructions. DNA was amplified by using the 341F-806R primer set (341F [CCTAYGGGRBGCASCAG] and 806R [GGAC-TACNNGGGGTATCTAAT]), which targeted the V3–V4 region of the bacterial 16S rDNA gene. PCR products were purified with the AxyPrepDNA Gel Extraction Kit (AXYGEN). Referring to the preliminary quantitative results of electrophoresis, the PCR amplified recovered products were detected and quantified with QuantiFluor™-ST Blue Fluorescence Quantification System (Promega), and mixed according to the sequencing amount required for each sample in the appropriate proportions. Library construction was performed using NEB Next® Ultra™DNA Library Prep Kit. The constructed libraries were QC'd by Agilent Bioanalyzer 2100 and Qubit, and then sequenced by Illumina NovaSeq PE250 after the libraries passed the QC.

## 2.3. Sequencing data analysis

Sequence analyses were performed using QIIME software [17], including the extraction of operational taxonomic units (OTUs),  $\alpha$  diversity analysis,  $\beta$  diversity analysis, linear discriminant analysis coupled with effect size (LDA Effect Size, LEfSe), and STAMP variance analysis, etc.  $\alpha$  diversity analyses included ACE, Chao1, Observed\_Species, Shannon, Simpson, and Coverage.  $\beta$  diversity analyses included Unweighted Pair-group Method with Arithmetic Mean (UPGMA), Principal Co-ordinates Analysis (PCoA), Principal Component Analysis (PCA), Non-Metric Multi-Dimensional Scaling (NMDS), and UniFrac analysis [18]. Differences in functionality between samples or subgroups were analyzed using PICRUST software. Differences in species diversity between groups were analyzed for significance by *t*-test and adonis test. LDA and Welch's *t*-test were used to identify bacterial species with significant differences in abundance between groups and for functional prediction.

## 2.4. Metabolomics data collection

After the sample was thawed slowly at  $4^{\circ}\text{C}$ , an appropriate amount of sample was added to pre-cooled methanol/acetonitrile/water solution (2:2:1, v/v), vortexed and mixed, sonicated at low temperature for 30 min, and then centrifuged at 14,000 g at  $4^{\circ}\text{C}$  for 20 min, and the supernatant was taken and vacuum-dried, and then 100  $\mu\text{L}$  of acetonitrile and water solution (acetonitrile:water = 1:1, v/v) was added to re-dissolve it for mass spectrometry analysis. For mass spectrometry analysis, 100  $\mu\text{L}$  of aqueous acetonitrile solution (acetonitrile:water = 1:1, v/v) was added and redissolved, vortexed, and centrifuged at 14,000 g for 15 min. The samples were separated on an Agilent 1290 Infinity LC ultra-high performance liquid chromatography system (UHPLC, AGILENT, USA) with a HILIC column; the column temperature was  $25^{\circ}\text{C}$ ; the flow rate was 0.5 mL/min; the injection volume was 2  $\mu\text{L}$ ; and the mobile phases were composed of A (PH = 9.5): water + 25 mM ammonium acetate + 25 mM ammonia, and B: acetonitrile. The gradient elution program was as follows: 0–0.5 min, 95 % B; 0.5–7 min, B varied linearly from 95 % to 65 %; 7–8 min, B varied linearly from 65 % to 40 %; 8–9 min, B was maintained at 40 %; 9–9.1 min, B varied linearly from 40 % to 95 %; 9.1–12 min, B was maintained at 95 %; throughout the analysis, B was maintained at 95 %. B was maintained at 95 % for 9.1–12 min; the samples were placed in the autosampler at  $4^{\circ}\text{C}$  during the whole analysis. The samples were analyzed in a  $4^{\circ}\text{C}$  autosampler throughout the analysis. To avoid the influence of fluctuations in the instrumental detection signal, the samples were analyzed continuously in a randomized order. An AB Triple TOF 6600 mass spectrometer was used to collect the primary and secondary spectra of the samples, and the ESI source conditions after HILIC chromatographic separation were as follows: Ion Source Gas1 (Gas1): 60, Ion Source Gas2 (Gas2): 60, Curtain gas (CUR): 30, source Temperature:  $600^{\circ}\text{C}$ , IonSapary Voltage Floating (ISVF)  $\pm 5500$  V (positive and negative modes); TOF MS scan *m/z* range: 60–1000 Da, product ion scan *m/z* range: 25–1000 Da, TOF MS scan accumulation time 0.20 s scan accumulation time 0.20 s/spectra, product ion scan accumulation time 0.05 s/spectra; the secondary mass spectra were obtained by information dependent acquisition (IDA), and the high sensitivity mode was used. The secondary mass spectra were obtained by information dependent acquisition (IDA) and adopted the high sensitivity mode, Declustering potential (DP):  $\pm 60$  V (positive and negative modes), Collision Energy:  $35 \pm 15$  eV, and the IDA settings were as follows Exclude isotopes within 4 Da, Candidate ions to Exclude isotopes within 4 Da, Candidate ions to monitor per cycle: 10 [19].

## 2.5. Metabolomics data analysis

The raw data in Wiff format were converted to mzXML format by ProteoWizard, and then XCMS software was used for peak alignment, retention time correction and extraction of peak areas. After the data were imported into SIMCA 14.1 software package, univariate and multidimensional statistical analyses were performed. Univariate statistical analyses included Fold Change Analysis (FC Analysis), T-test. Multidimensional statistical analysis included PCA, Partial Least Squares Discriminant Analysis (PLS-DA), and Orthogonal Partial Least Squares Discriminant Analysis (OPLS-DA) to show differences between groups, and the parameters  $R^2Y$  and  $Q^2$  were used to assess the robustness and predictive ability of the model. Variable-importance projection (VIP) values exceeding 1.0 were selected as a proxy for changing metabolites, and then the remaining variables were assessed using *t*-tests. In addition, metabolic

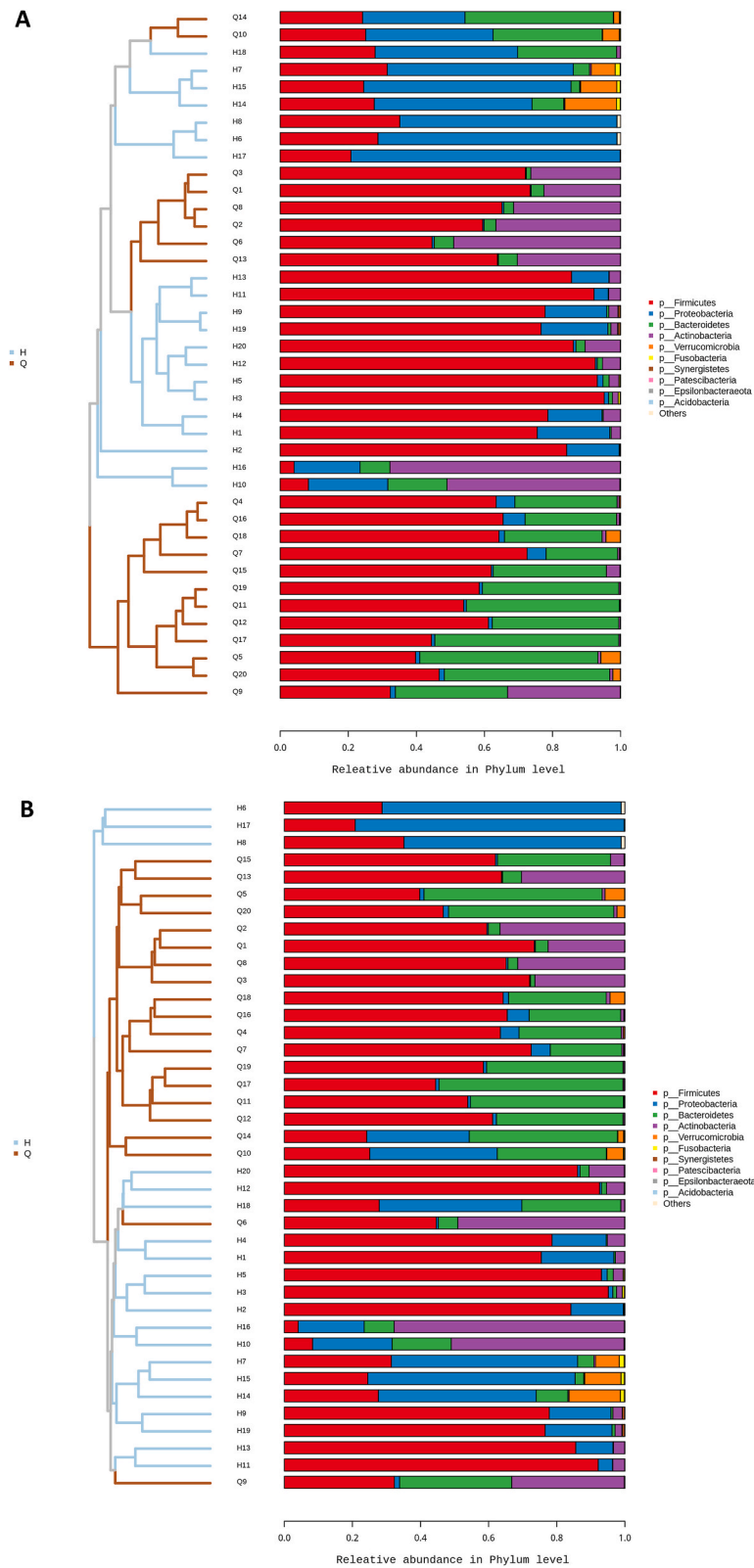


**Fig. 1.** Species composition analysis. **A** UPGMA cluster tree and community structure histogram based on Weighted Unifrac distance. **B** UPGMA cluster tree and community structure histogram based on Unweighted Unifrac distance.

pathways were searched using the KEGG (<http://www.genome.jp/kegg/>) database and the COG (<https://www.ncbi.nlm.nih.gov/research/cog/>) database [20].

2.6. Flora-metabolite correlation analysis

The correlation coefficients between the screened significantly different flora and significantly different metabolites in the experimental samples were analyzed by using Spearman statistics and combined with hierarchical clustering and scatter plot analysis in R language.

2.7. Statistical analyses

Data comparing the two groups were analyzed using *t*-test (SPSS 26). Clinical characterization was done using Fisher's exact test and Welch *t* test where appropriate, *p*-value less than 0.05 was considered statistically significant.

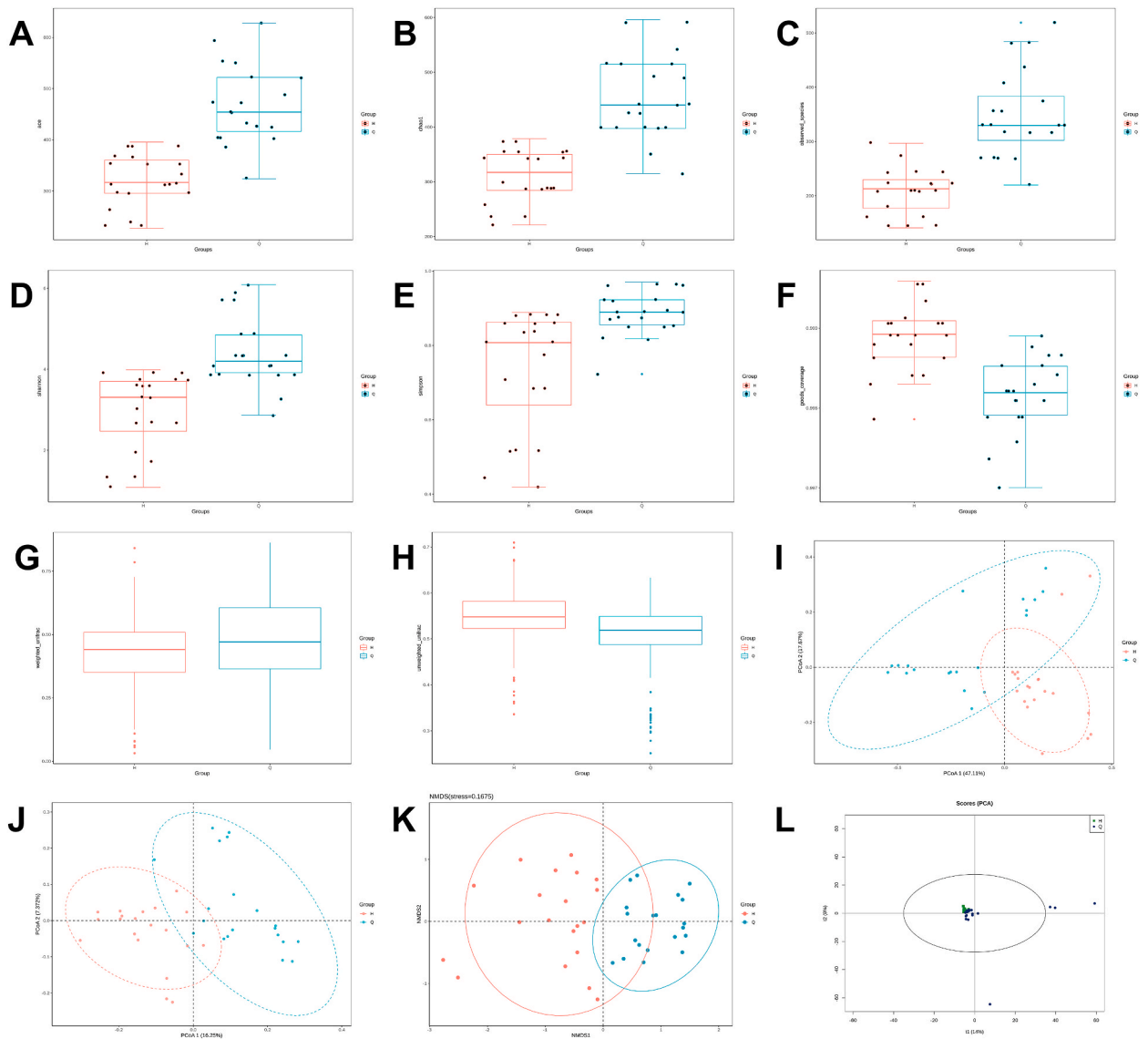


**Fig. 2.**  $\alpha$  diversity analysis and  $\beta$  diversity analysis. A-F Box plots of inter-group differences in  $\alpha$ -diversity indices (ACE, Chao1, Observed\_Species, Shannon, Simpson, Coverage). G, H Intergroup variance analysis of  $\beta$  diversity based on Weighted Unifrac and Unweighted Unifrac distances. I, J PCoA based on Weighted Unifrac and Unweighted Unifrac distances. K NMDS analysis. L Principal component analysis.

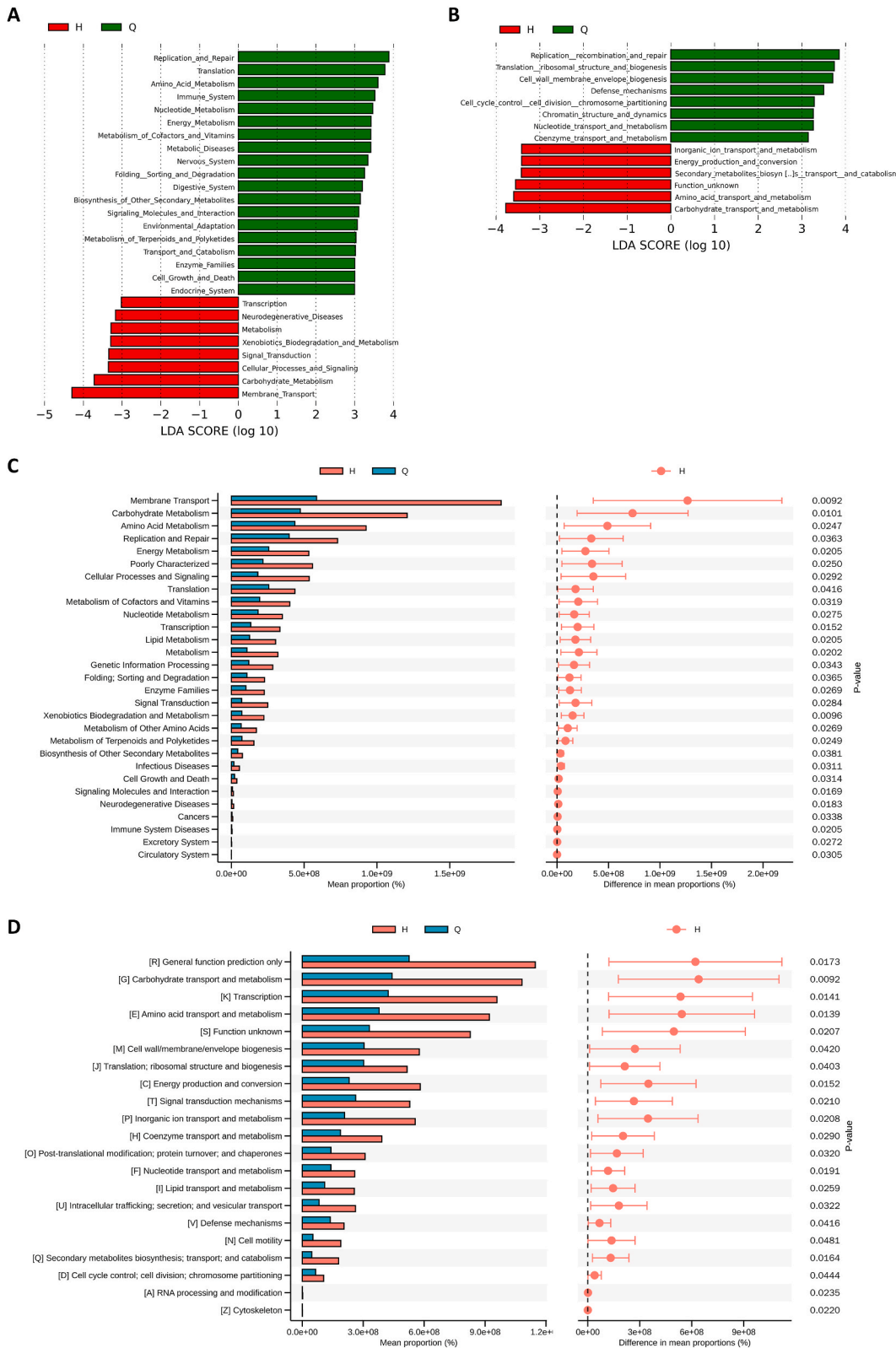


**Fig. 3.** Differential species functional prediction. A, B LefSe analysis based on KEGG and COG functional prediction. C, D STAMP differential analysis based on KEGG and COG functional prediction. p (Welch's *t*-test) < 0.05, indicating significant differences.

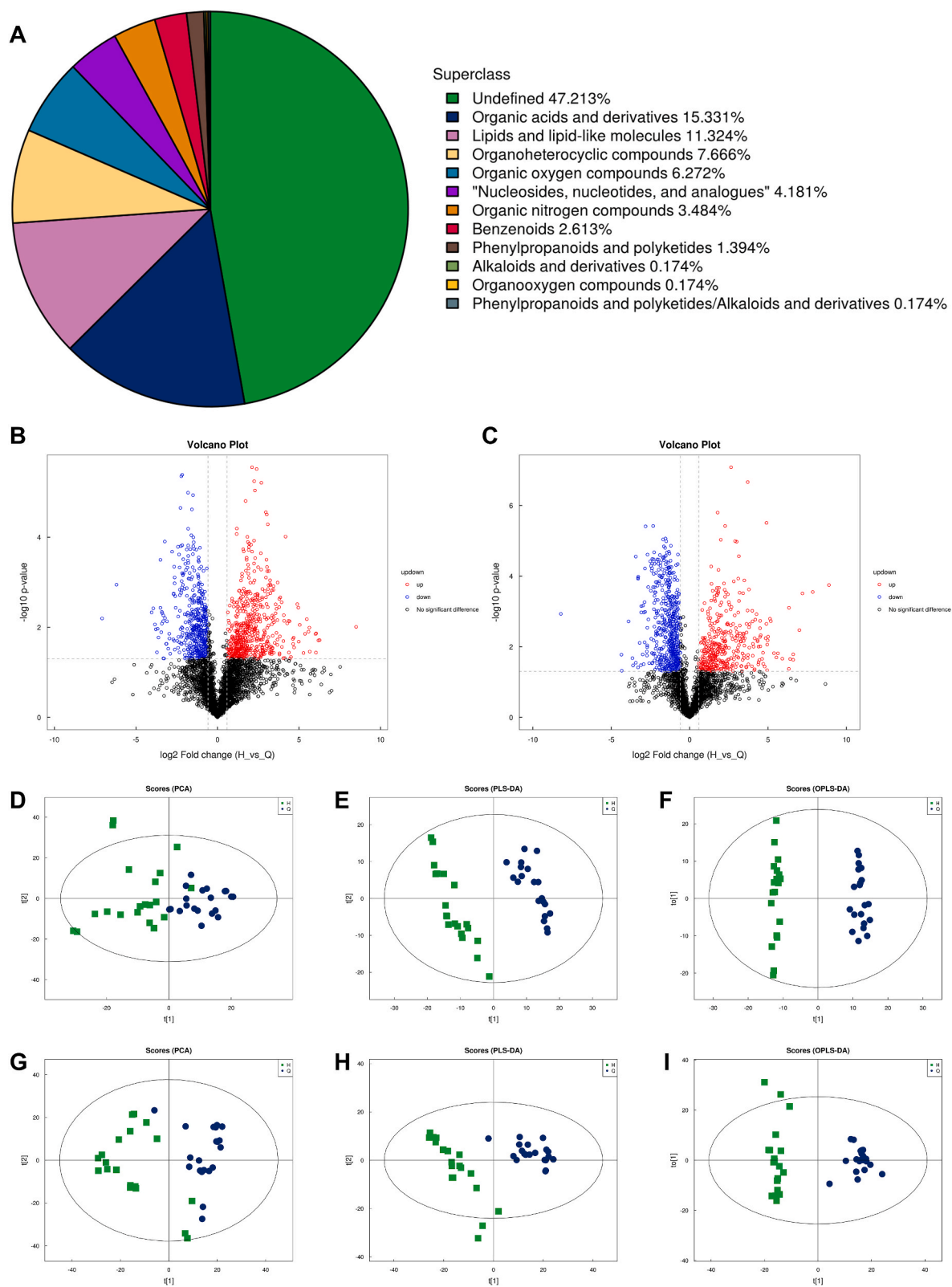


**Fig. 4.** Metabolite classification and analysis of differences between groups. **A** Statistical plot of metabolite classification. **B, C** Plots of positive and negative ion mode volcanoes. **D, G** Plots of positive and negative ion mode PCA scores. **E, H** Plots of positive and negative ion mode PLS-DA scores. **F, I** Plots of positive and negative ion mode OPLS-DA scores.

### 3. Results

#### 3.1. Differential microbiome detection

Clean reads of all samples were clustered and sequences were clustered into OTUs with 97 % agreement, and then the representative sequences of OTUs were annotated with species. The results showed a total of 692 OTUs in both groups, 554 unique to group Q and 146 unique to group H. The species composition of the samples was analyzed using community structure component maps and UPGMA clustering trees (Fig. 1A and B), and it was found that there were significantly different species and clustering between the same groups in the two groups, implying that there were significant differences in the intestinal flora of patients before and after pancreaticoduodenectomy. To assess the differences in bacterial diversity between the two groups, we performed  $\alpha$  diversity analysis (Fig. 2A–F), which showed that the diversity and richness of the intestinal flora in group Q was significantly higher than that in group H. We next assessed the compositional variability of the flora between groups using  $\beta$ -diversity analysis (Fig. 2G–L), and the results suggested that the two groups of samples differed in the overall flora structure. The significance of the differences in community

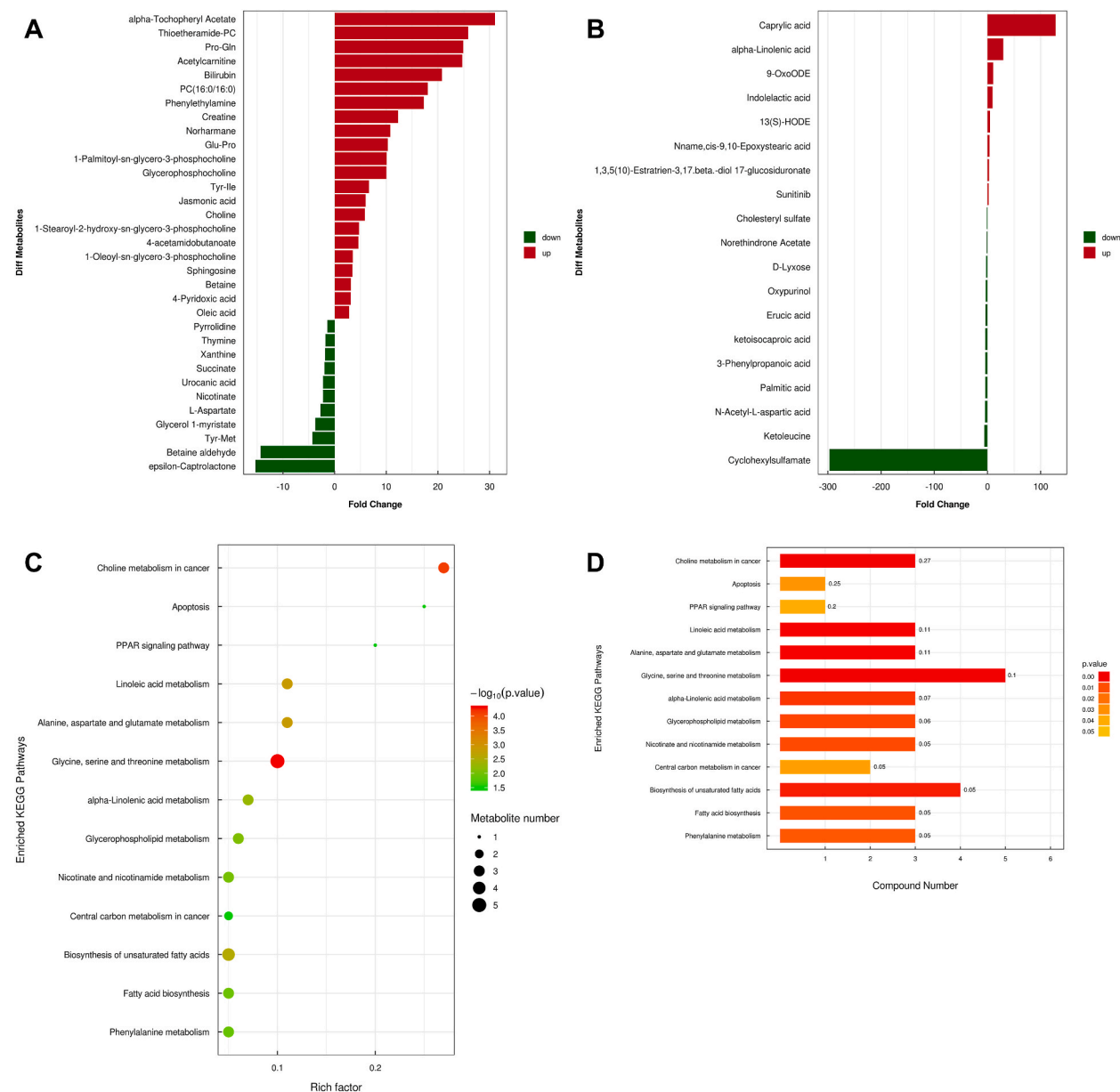


**Fig. 5.** Differential metabolite and functional analysis. A, B Positive and negative ion pattern significant difference metabolite expression differential multiplicity analysis. C, D KEGG enrichment pathway diagram.



**Fig. 6.** Spearman correlation analysis hierarchical clustering heat map. Red indicates positive correlation, blue indicates negative correlation, darker the color the stronger the correlation. \* indicates  $p < 0.05$ ; \*\* indicates  $p < 0.01$ ; \*\*\* indicates  $p < 0.001$ .

structure between groups was further tested and the results showed significant differences between groups (adonis:  $R^2 = 0.144$ ,  $P < 0.05$ ).

We next applied LEfSe analysis and STAMP difference analysis to screen for species that differed between groups ( $LDA > 2$ ,  $P < 0.05$ ). The results showed that group Q was enriched in Bacteroides, Prevotella, Faecalibacterium, and Subdoligranulum; while group H was enriched in klebsiella and Lachnocostridium (Supplemental Fig. 1). Further functional prediction and differential functional analysis of the samples showed significant differences in functional entries such as membrane transport, glucose metabolism, energy metabolism, amino acid metabolism, and cellular signaling between the groups (Fig. 3A–D).

### 3.2. Differential metabolite detection

In this part of the experiment, we identified 405 metabolites in positive ion mode and 169 metabolites in negative ion mode and categorized the statistics according to their chemical classification attribution information (Fig. 4A). All metabolites detected in positive and negative ion modes were first analyzed for differences based on univariate analysis. Differential metabolites with  $FC > 1.5$

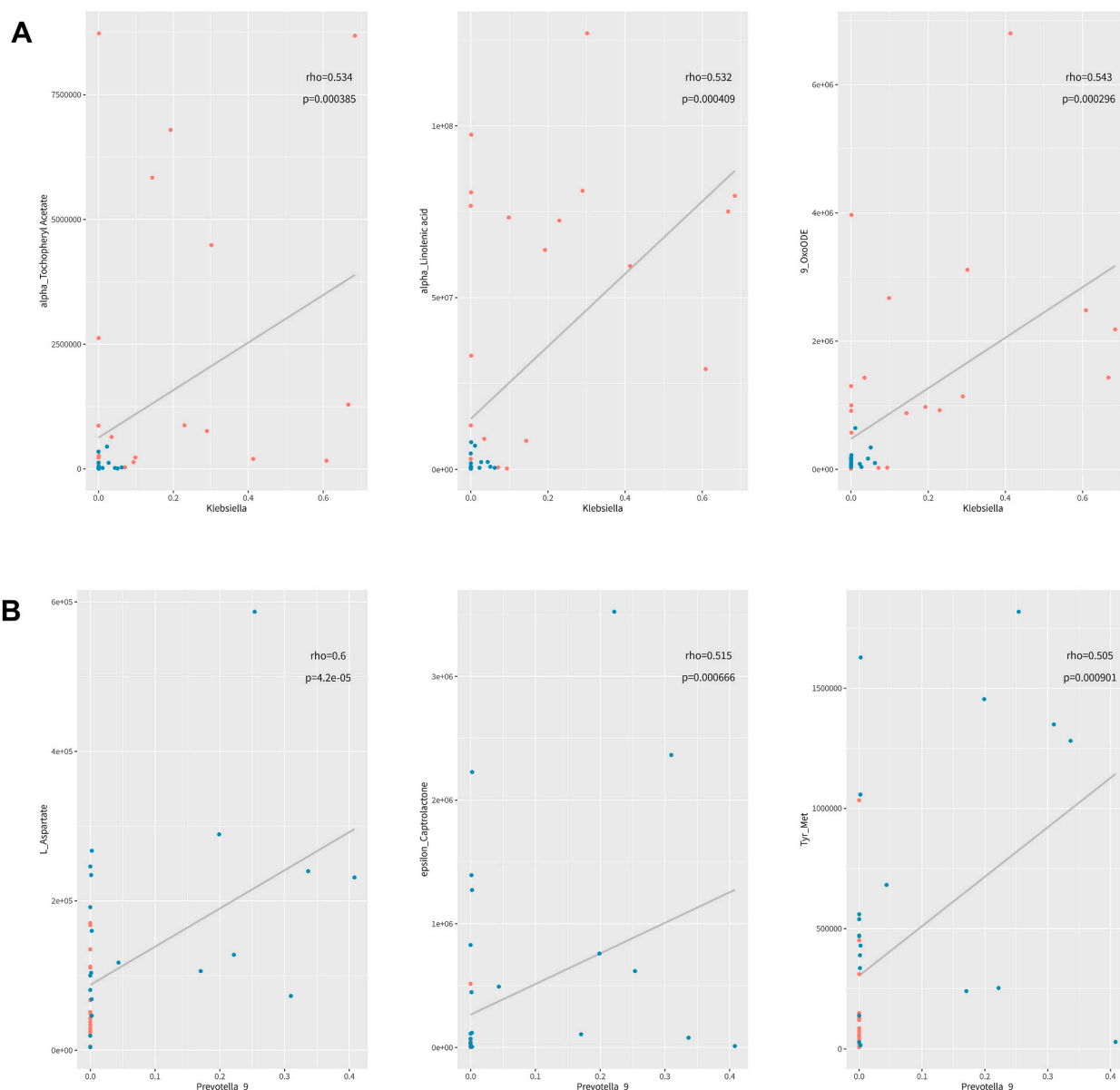


**Fig. 7.** Differential microbe-metabolite correlation analysis. **A** Scatter plot of klebsiella correlations. **B** Scatter plot of Prevotella correlations. The rho is the spearman correlation coefficient between the relative abundance of the flora and the metabolite intensity value, and the p-value is the level of significance of this rho.

or  $FC < 0.67$ ,  $p < 0.05$ , were visualized using volcano plots (Fig. 4B and C). We next used multidimensional statistical analysis to reflect the differences between groups at the overall level as well as to reflect the variability within groups. The results showed a clear clustering between individual samples of the same group and a more pronounced gap between the two groups, which can be considered as a difference in the overall metabolite structure between the two groups (Fig. 4D–I).

Combining the data from the above two analytical methods, the differential metabolites were further screened ( $VIP > 1$ ,  $P < 0.05$ ) and made into bar charts, which showed that the main differential metabolites were: benzenoids, lipids and lipid-like molecules, nucleosides nucleotides and analogues, organic acids and derivatives, organic oxygen compounds, organoheterocyclic compounds, phenylpropanoids and polyketides (Fig. 5A and B and Supplemental Tables 1 and 2). The screened significantly different metabolites were further analyzed. These metabolites were mapped to approximately 60 different KEGG metabolic pathways, with 13 KEGG metabolic pathways having a number of differential metabolites greater than five (Fig. 5C and D).

### 3.3. Differential microbe-metabolite correlation analysis

The data measured in the above two parts of the experiment were used as the basis for the subsequent analysis. We found 88 significantly positively correlated and 69 negatively correlated microbe-metabolite pairs ( $P < 0.05$ ,  $0.5 < IRI < 1$ ), calculated by Spearman analysis (Fig. 6). Further analysis of these microbe-metabolite pairs revealed that *klebsiella* showed an elevated trend with  $\alpha$  tocopheryl acetate,  $\alpha$ -linolenic acid, and 9-oxoode in the postoperative period (Fig. 7A). In contrast, *Prevotella* with L-aspartate, epsilon-caprolactone, and tyr-met all showed a decreasing trend in the postoperative period (Fig. 7A).

## 4. Discussion

Gastrointestinal reconstruction after pancreaticoduodenectomy fundamentally alters oxygen utilization, intestinal pH, and food transit time, thus also altering the microbes and metabolites of the gut.

By  $\alpha$  diversity analysis (Fig. 2A–F), we learned that the diversity and abundance of the flora in group Q was significantly higher than that in group H. This may have occurred due to partial inhibition of the flora by antibiotics as a result of the patients' postoperative antibiotic use, and the low abundance of intestinal flora may have led to postoperative complications [21]. Further screening for species that differed between groups, we found a variety of interesting genera (Supplemental Fig. 1).

Related studies have shown that *klebsiella* is a common cause of healthcare-associated infections and that patients are often infected by intestinal colonizing strains [22,23]. And the risk of infection depends on the amount of *klebsiella* in the gut, independent of the type of *klebsiella* [24,25], but there is a class of genes that increase the intestinal fitness of the microbiome and thus the intestinal abundance of the microbiome [26], and *klebsiella* with such genes are likely to cause the greatest risk of infection in patients. The significantly elevated *klebsiella* in the intestine of patients after pancreaticoduodenectomy and its important role in the stool of postoperative patients greatly increases the incidence of postoperative infections with colonized strains of intestinal bacteria.

*Lachnoclostridium* is a new species identified from the human intestinal microbiota in recent years [27]. Related studies have demonstrated that *Lachnoclostridium* may be a novel faecal marker that can be used for the diagnosis of colorectal adenomas and cancers [28,29]. In our trial, patients had significantly elevated *Lachnoclostridium* postoperatively, and we have reason to believe that this would lead to an increased chance of colorectal adenomas and cancers in patients after surgery.

*Bifidobacterium* has functions such as promoting the digestion and absorption of nutrients and enhancing human resistance [30]. Foods containing *Bifidobacterium* such as yogurt and cheese can form biofilms in the human intestine to prevent the adhesion and invasion of pathogenic bacteria, and *Bifidobacterium* can induce apoptosis and inhibit the invasiveness of cancer cells, which helps the body fight against cancer [31]. *Prevotella* is considered the next generation of probiotics, which can effectively inhibit the colonization and growth of pathogenic microorganisms through the interaction of the immune system and microbiota, while also promoting glucose metabolism and regulating heart function [32]. *Bacteroides* is a dominant genus in the human intestinal flora, accounting for approximately 25 % of the overall microorganisms [33]. They can establish a long-term stable symbiotic relationship with their hosts and produce a variety of metabolites that can control the development of disease [34]. For example, propionates can prevent the development of gastrointestinal tumors by inducing apoptosis of tumor cells [35]. Butyrate plays an important role in maintaining and protecting intestinal barrier function [36].

All of these probiotics showed a decreasing trend after surgery, with a significant decrease in the promotion effect produced by probiotics, and the microenvironmental disturbances caused by surgery resulted in changes in the dominant intestinal microbiome and dysbiosis, which further led to a decrease in probiotics and an increase in pathogenic bacteria, which in turn led to various postoperative complications and aggravation of the disease. Several studies have shown that postoperative administration of probiotics can help regulate intestinal flora, reduce inflammatory responses, and improve the mucosal barrier in patients with gastrointestinal malignancies [37–39]. The regulation of intestinal flora improves the postoperative treatment outcome and reduces the incidence of tumor recurrence. At the same time, we also need to enhance postoperative review monitoring of patients, such as endoscopy, for early detection of possible colorectal adenomas and cancers.

Metabolically, group H rich in amines, organic acids, and fatty acids (Fig. 5A and B), suggesting that postoperative patients' intestines do not maintain carbohydrate metabolism and a more reducible environment in the intestine well. In addition to this, studies have shown that gastrointestinal tumor cancer cells exhibit high glutaminase activity and lead to the conversion of glutamine to glutamate [40]. In our experiment, however, both glutamine and glutamate levels were elevated in the patients after surgery, but the glutamine elevation was more pronounced, probably due to the reduction of glutaminase activity after tumor resection. If the glutamine level remained low after surgery, it indicates that the glutaminase activity is high, which may suggest that the tumor was not

completely resected and the prognosis is poor.

We next examined 13 KEGG metabolic pathways and found that activated choline metabolism is a hallmark of tumorigenesis and progression (Fig. 5C and D), with elevated levels of choline phosphate and glycerophosphorylcholine found in the majority of cancers tested to date [41]. Choline, a major component of biofilms, is consumed in large quantities during tumor cell proliferation to supply cellular needs [42]. In our experiment, the elevated choline metabolism level of the patient after surgery, combined with the characteristics of periampullary carcinoma prone to early metastasis, was considered as early micro-metastases, which became active by the stimulation of surgery, and it may be used as a potential marker to judge the prognosis of the patient. The faecal metabolome is the result of the interaction of genetic, environmental and nutritional variables, unlike histological techniques that employ biological fluids such as serum and urine. Therefore, it may be more effective to use metabolomics that includes faecal to discover biomarkers [40].

There is also a potential link between intestinal microbiome and metabolites, in this experiment *Klebsiella* with  $\alpha$  tocopheryl acetate,  $\alpha$ -linolenic acid, and 9-oxoode all tended to be elevated postoperatively (Fig. 7A). *Klebsiella* increases the chance of postoperative infection [43], while at the same time all of these metabolites have some anti-inflammatory effect [44], and their elevated levels may be related to the body's immune response to postoperative inflammation. In contrast, *Prevotella*, along with L-aspartate, epsilon-caprolactone, and Tyr-met, showed a decreasing trend in the postoperative period (Fig. 7B), which indicates that the decrease in the abundance of such probiotics as *Prevotella* in the intestine will affect the amino acid metabolism in the gut to some extent.

Although our analysis is data-driven, further validation is needed. In addition, our patients' gastrointestinal reconstructions were all gastrojejunal anastomotic, so our findings may represent this specific reconstruction. We acknowledge some limitations of our study, but open new avenues for improving patient prognosis. Overall, our experiment revealed unique and different characteristics of intestinal microbiome and metabolites in patients before and after pancreaticoduodenectomy.

#### Ethics statement

The samples and clinical information used in this study were obtained under conditions of informed consent and with approval by 900th Hospital of Joint Logistics Support Force of People's Liberation Army (2021–022).

#### Funding statement

This work was supported by 900th Hospital of Joint Logistics Support Force of People's Liberation Army (2020L01).

#### Data availability statement

Data included in article/supplementary material/referenced in article.

#### CRediT authorship contribution statement

**Junwei Fang:** Writing – review & editing, Writing – original draft, Visualization, Validation, Software, Methodology, Investigation, Formal analysis, Data curation. **Chunhong Xiao:** Writing – review & editing, Supervision, Resources, Project administration, Methodology, Investigation, Funding acquisition, Data curation, Conceptualization. **Yafeng Qi:** Supervision, Resources, Conceptualization. **Weixuan Hong:** Visualization, Investigation, Data curation. **Meiping Wang:** Writing – review & editing, Supervision, Resources, Project administration, Funding acquisition, Conceptualization.

#### Declaration of competing interest

The authors declare that they have no known competing financial interests or personal relationships that could have appeared to influence the work reported in this paper.

#### Acknowledgments

The authors would like to thank the staff of the General Surgery Department of 900th Hospital of Joint Logistics Support Force of People's Liberation Army for their help.

#### Appendix A. Supplementary data

Supplementary data to this article can be found online at <https://doi.org/10.1016/j.heliyon.2024.e24393>.

## References

- [1] K. Guyton, J.C. Alverdy, The gut microbiota and gastrointestinal surgery, *Nat Rev Gastroenterol Hepatol* 14 (2017) 43–54. <https://doi.org/10.1038/nrgastro.2016.139>.
- [2] A.K. Lederer, P. Pisarski, L. Kousoulas, S. Fichtner-Feigl, R. Huber, Postoperative changes of the microbiome: are surgical complications related to the gut flora? A systematic review, *BMC Surg.* 17 (2017).
- [3] C. Gutiérrez-Repiso, I. Moreno-Indias, A.D. Hollanda, G.M. Martín-Núñez, F.J. Tinahones, Gut microbiota specific signatures are related to the successful rate of bariatric surgery, *Am. J. Transl. Res.* 11 (2019) 942–952.
- [4] S. Mondot, P. Lepage, P. Seksik, M. Allez, P.F. Marteau, Structural robustness of the gut mucosal microbiota is associated with Crohn's disease remission after surgery, *Gut* 65 (2015) [gutjnl-2015-309184](https://doi.org/10.1136/gutjnl-2015-309184).
- [5] C.C. Vining, K. Kuchta, D. Schuitemoeder, P. Paterakos, Y. Berger, K.K. Roggin, M.S. Talamonti, M.E. Hogg, Risk factors for complications in patients undergoing pancreaticoduodenectomy: A NSQIP analysis with propensity score matching, *J Surg Oncol* 122 (2020) 183–194. <https://doi.org/10.1002/jso.25942>.
- [6] X.-H. Lin, K.-H. Huang, W.-H. Chuang, J.-C. Luo, C.-C. Lin, P.-H. Ting, S.-H. Young, W.-L. Fang, M.-C. Hou, F.-Y. Lee, The long term effect of metabolic profile and microbiota status in early gastric cancer patients after subtotal gastrectomy, *PLoS One* 13 (2018) e0206930, <https://doi.org/10.1371/journal.pone.0206930>.
- [7] Wool Bang, Hyuk-Joon Eom, Moon-Won Lee, Jae Yoo, Cho Jin, Synchronous and metachronous cancers in patients with gastric cancer, *J. Surg. Oncol.* 98 (2008) 106–110.
- [8] Y. Ikeda, M. Saku, H. Kawanaka, M. Nonaka, K. Yoshida, Features of second primary cancer in patients with gastric cancer, *Oncology* 65 (2003) 113–117.
- [9] J.H. Kim, M.-J. Kim, J.-J. Chung, W.J. Lee, H.S. Yoo, J.T. Lee, Differential diagnosis of periampullary carcinomas at MR imaging, *Radiographics* 22 (2002) 1335–1352, <https://doi.org/10.1148/rg.226025060>.
- [10] 赵闯, 戴朝六, 提高壶腹周围癌术前定性诊断的方法及意义, *肝胆外科杂志.* 26 (2018) 245–250.
- [11] 唐文皓, 唐健雄, 袁祖荣, 胰头癌外科治疗中应注意的几个问题, *国际外科学杂志.* 46 (2019) 5.
- [12] Z. Xie, X. Chen, J. Li, Y. Guo, H. Li, X. Pan, J. Jiang, H. Liu, B. Wu, Salivary HOTAIR and PVT1 as novel biomarkers for early pancreatic cancer, *Oncotarget* 7 (2016) 25408–25419, <https://doi.org/10.18632/oncotarget.8323>.
- [13] M. Humeau, A. Vignolle-Vidoni, F. Sicard, F. Martins, B. Bournet, L. Buscail, J. Torrisani, P. Cordelier, K. Jeyaseelan, Salivary MicroRNA in pancreatic cancer patients, *PLoS One* 10 (2015) e0130996–e0130996, <https://doi.org/10.1371/journal.pone.0130996>.
- [14] N.A. Victoria, M. Kim, Early detection of pancreatic cancer, *Chin. J. Cancer Res.* 4 (2015) 11–21.
- [15] M.D. Angelis, G. Garruti, F. Minervini, L. Bonfrate, P. Portincasa, M. Gobetti, The food-gut human axis: the effects of diet on gut microbiota and metabolome, *Curr. Med. Chem.* 24 (2017).
- [16] T. Hank, U. Klaiher, K. Sahara, M. Schindl, O. Strobel, Chirurgie periampullärer pankreaskarzinome, *Chir* 92 (2021) 776–787, <https://doi.org/10.1007/s00104-021-01462-1>.
- [17] J.G. Caporaso, J. Kuczynski, J. Stombaugh, K. Bittinger, F.D. Bushman, E.K. Costello, N. Fierer, A.G. Peña, J.K. Goodrich, J.I. Gordon, G.A. Huttley, S.T. Kelley, D. Knights, J.E. Koenig, R.E. Ley, C.A. Lozupone, D. McDonald, B.D. Muegge, M. Pirrung, J. Reeder, J.R. Sevinsky, P.J. Turnbaugh, W.A. Walters, J. Widmann, T. Yatsunenko, J. Zaneveld, R. Knight, QIIME allows analysis of high-throughput community sequencing data, *Nat. Methods* 7 (2010) 335–336, <https://doi.org/10.1038/nmeth.f.303>.
- [18] E. Avershina, T. Frisli, K. Rudi, De novo semi-alignment of 16S rRNA gene sequences for deep phylogenetic characterization of next generation sequencing data, *Microb. Environ.* 28 (2013) 211–216, <https://doi.org/10.1264/jsmc2.me12157>.
- [19] S. Cheng, X. Ma, S. Geng, X. Jiang, Y. Li, L. Hu, J. Li, Y. Wang, X. Han, Fecal microbiota transplantation beneficially regulates intestinal mucosal autophagy and alleviates gut barrier injury, *mSystems* 3 (2018), <https://doi.org/10.1128/mSystems.00137-18>.
- [20] X. Zhou, L. Liu, X. Lan, D. Cohen, Y. Zhang, A.V. Ravindran, S. Yuan, P. Zheng, D. Coghill, L. Yang, S.E. Hetrick, X. Jiang, J.-J. Benoliel, A. Cipriani, P. Xie, Polyunsaturated fatty acids metabolism, purine metabolism and inosine as potential independent diagnostic biomarkers for major depressive disorder in children and adolescents, *Mol. Psychiatr.* 24 (2019) 1478–1488, <https://doi.org/10.1038/s41380-018-0047-z>.
- [21] V. Pascal, M. Pozuelo, N. Borrue, F. Casellas, D. Campos, A. Santiago, X. Martínez, E. Varela, G. Sarrabayrouse, K. Machiels, S. Vermeire, H. Sokol, F. Guarner, C. Manichanh, A microbial signature for Crohn's disease, *Gut* 66 (2017) 813–822, <https://doi.org/10.1136/gutjnl-2016-313235>.
- [22] K. Rao, A. Patel, Y. Sun, J. Vornhagen, J. Motyka, A. Collingwood, A. Teodorescu, J.H. Baang, L. Zhao, K.S. Kaye, M.A. Bachman, Risk factors for Klebsiella infections among hospitalized patients with preexisting colonization, *mSphere* 6 (2021), <https://doi.org/10.1128/mSphere.00132-21>.
- [23] D. Li, X. Huang, H. Rao, H. Yu, S. Long, Y. Li, J. Zhang, Klebsiella pneumoniae bacteremia mortality: a systematic review and meta-analysis, *Front. Cell. Infect. Microbiol.* 13 (2023) 1157010, <https://doi.org/10.3389/fcimb.2023.1157010>.
- [24] R.M. Martin, J. Cao, S. Brisse, V. Passet, W. Wu, L. Zhao, P.N. Malani, K. Rao, M.A. Bachman, Molecular epidemiology of colonizing and infecting isolates of Klebsiella pneumoniae, *mSphere* 1 (2016) e00261-16, <https://doi.org/10.1128/mSphere.00261-16>.
- [25] C.L. Gorrie, M. Mirjana, R.R. Wick, D.J. Edwards, N.R. Thomson, R.A. Strugnell, N.F. Pratt, J.S. Garlick, K.M. Watson, D.V. Pilcher, Gastrointestinal carriage is a major reservoir of Klebsiella pneumoniae infection in intensive care patients, *Clin. Infect. Dis.* (2017) 208.
- [26] R.M. Martin, J. Cao, W. Wu, L. Zhao, D.M. Manthei, P. Ali, S. Evan, P.N. Malani, K. Rao, M.A. Bachman, Identification of pathogenicity-associated loci in Klebsiella pneumoniae from hospitalized patients, *mSystems* 3 (2018) e00015-18.
- [27] S. Brahimi, F. Cadoret, P.E. Fournier, V. Moal, D. Raoult, "Lachnoclostridium urinimassiliense" sp. nov. and sp. nov., two new bacterial species isolated from human urine after kidney transplantation, *New Microbes New Infect* 16 (2017) 73–75, <https://doi.org/10.1016/j.nmni.2017.01.008>.
- [28] N. Hasan, H. Yang, Factors affecting the composition of the gut microbiota, and its modulation, *PeerJ* 7 (2019) 31.
- [29] P.P. Erawijantari, S. Mizutani, H. Shirota, S. Shiba, T. Nakajima, T. Sakamoto, Y. Saito, S. Fukuda, S. Yachida, T. Yamada, Influence of gastrectomy for gastric cancer treatment on faecal microbiome and metabolome profiles, *Gut* 69 (2020) 1404–1415, <https://doi.org/10.1136/gutjnl-2019-319188>.
- [30] 刘梦瑶, 阳田恬, 闫晓松, 程强, 陈露瑶, 张静, 华正昌, 张日俊, 双歧杆菌及其后生素的益生功能与应用, *饲料工业.* 2022, pp. 1–6.
- [31] J. An, H. Kim, K.M. Yang, An aqueous extract of a Bifidobacterium species induces apoptosis and inhibits invasiveness of non-small cell lung cancer cells, *J. Microbiol. Biotechnol.* 30 (2020) 885–893, <https://doi.org/10.4014/jmb.1912.12054>.
- [32] F. Huang, R.R.R. Sardari, A. Jasilionis, O. Böök, R. Öste, A. Rascón, L. Heyman Lindén, O. Holst, E.N. Karlsson, Cultivation of the gut bacterium Prevotella copri DSM 18205T using glucose and xylose as carbon sources, *MicrobiologyOpen* 10 (2021), <https://doi.org/10.1002/mbo3.1213>.
- [33] J. Ochoa-Repáraz, D.W. Mielcarz, Y. Wang, S. Begum-Haque, S. Dasgupta, D.L. Kasper, L.H. Kasper, A polysaccharide from the human commensal Bacteroides fragilis protects against CNS demyelinating disease, *Mucosal Immunol.* 3 (2010) 487–495.
- [34] J.J. Faith, J.L. Guruge, M. Charbonneau, S. Subramanian, H. Seedorf, A.L. Goodman, J.C. Clemente, R. Knight, A.C. Heath, R.L. Leibel, The long-term stability of the human gut microbiota, *Science* 341 (2013) 1237439.
- [35] R.K. Cruz-Bravo, R.G. Guevara-González, M. Ramos-Gómez, B.D. Oomah, P. Wiersma, R. Campos-Vega, G. Loarca-Pi A, The fermented non-digestible fraction of common bean (Phaseolus vulgaris L.) triggers cell cycle arrest and apoptosis in human colon adenocarcinoma cells, *Genes Nutr* 9 (2014) 359, 4.
- [36] E.E. Elamin, A.A. Masclee, J. Dekker, H.J. Pieters, D.M. Jonkers, Short-chain fatty acids activate AMP-activated protein kinase and ameliorate ethanol-induced intestinal barrier dysfunction in Caco-2 cell monolayers, *J. Nutr.* 143 (2013) 1872–1881.
- [37] 李灼非, 邓兴明, 李粤, 吕国庆, 益生菌对结肠癌化疗及术后肠道菌群变化的影响以及与免疫功能下降的关系的研究, *贵州医药.* 42 (2018) 3.
- [38] F. Huang, S. Li, W. Chen, Y. Han, Y. Yao, L. Yang, Q. Li, Q. Xiao, J. Wei, Z. Liu, T. Chen, X. Deng, Postoperative probiotics administration attenuates gastrointestinal complications and gut microbiota dysbiosis caused by chemotherapy in colorectal cancer patients, *Nutrients* 15 (2023), <https://doi.org/10.3390/nu15020356>.
- [39] Y. Chen, A. Qi, D. Teng, S. Li, Y. Yan, S. Hu, X. Du, Probiotics and synbiotics for preventing postoperative infectious complications in colorectal cancer patients: a systematic review and meta-analysis, *Tech. Coloproctol.* 26 (2022) 425–436, <https://doi.org/10.1007/s10151-022-02585-1>.

- [40] Y. Yang, B.B. Misra, L. Liang, D. Bi, W. Weng, W. Wu, S. Cai, H. Qin, A. Goel, X. Li, Y. Ma, Integrated microbiome and metabolome analysis reveals a novel interplay between commensal bacteria and metabolites in colorectal cancer, *Theranostics* 9 (2019) 4101–4114, <https://doi.org/10.7150/thno.35186>.
- [41] K. Sonkar, V. Ayyappan, C.M. Tressler, O. Adelaja, R. Cai, M. Cheng, K. Glunde, Focus on the glycerophosphocholine pathway in choline phospholipid metabolism of cancer, *NMR Biomed.* 32 (2018), <https://doi.org/10.1002/nbm.4112>.
- [42] D. Gallego-Ortega, A. Ramirez De Molina, M.A. Ramos, F. Valdes-Mora, M.G. Barderas, J. Sarmentero-Estrada, J.C. Lecal, Differential role of human choline kinase alpha and beta enzymes in lipid metabolism: implications in cancer onset and treatment, *PLoS One* 4 (2009) e7819, <https://doi.org/10.1371/journal.pone.0007819>.
- [43] W. Li, L. Xu, H. Zhao, S. Zhu, Analysis of clinical distribution and drug resistance of klebsiella pneumoniae pulmonary infection in patients with hypertensive intra cerebral hemorrhage after minimally invasive surgery, *Pakistan J. Med. Sci.* 38 (2022) 237–242, <https://doi.org/10.12669/pjms.38.1.4439>.
- [44] G. Andres Contreras, J. De Koster, J. de Souza, J. Laguna, V. Mavangira, R.K. Nelli, J. Gandy, A.L. Lock, L.M. Sordillo, Lipolysis modulates the biosynthesis of inflammatory lipid mediators derived from linoleic acid in adipose tissue of periparturient dairy cows, *J. Dairy Sci.* 103 (2020) 1944–1955, <https://doi.org/10.3168/jds.2019-17256>.